

On Modelling of Maximum Electromagnetic Field in Electrically Large Enclosures

Dan Chen¹, Peng Hu², Zhongyuan Zhou², Xiang Zhou², Shouyang Zhai¹, Yan Chen¹

¹State Key Laboratory of Nuclear Power Safety Monitoring Technology and Equipment, Longcheng road, No. 441, 518172, Shenzhen, China, chendants@cgnpc.com.cn

²Research Center for Electromagnetic Environmental Effects, Southeast University, SEU road, No. 2, 211189, Nanjing, China, hfut_hupeng@126.com

Abstract: The maximum electromagnetic field formed in the electrically large enclosures for a given input power has always been the focus of electromagnetic compatibility issues such as radiation sensitivity and shielding effectiveness. To model the maximums in a simple manner, the electrically large enclosure can be regarded as a reverberation chamber (RC), thus the generalized extreme value (GEV) theory based framework is used for both undermoded and overmoded frequencies. Since the mechanical stirrer is not easy to be installed like that for RC, frequency stirring and mechanical stirring related configurations are discussed, and the corresponding results have confirmed the validity of frequency stirring with the estimate of the parameters in GEV distribution. As for the maximum field, a comparison has been made between GEV distribution and IEC 61000-4-21, and the corresponding results have also highlighted that the maximum field can be assessed by frequency stirring configuration, and by GEV distribution with a desired confidence.

Keywords: Maximum electromagnetic field, electromagnetic compatibility, electrically large enclosure, reverberation chamber, generalized extreme value distribution.

1. INTRODUCTION

With exploding applications of high-power and high-frequency electronics in different areas, e.g., ships, aircraft, and electric vehicles, the electromagnetic compatibility (EMC) related issues have attracted the interest of the EMC community. For high frequencies (i.e., high mode densities), the sensitive electronics inside metallic enclosures may be threatened by the potential risks from electromagnetic interference (EMI) with apertures, cables, or antennas. To solve EMC problems as well as to enable reliable operation of the sensitive electronics, it is necessary to have an *a priori* knowledge about the maximum field formed in these enclosures.

Fortunately, the well-established theory for reverberation chambers (RCs), or for the general case of electrically large enclosures (supporting several field modes at the lowest frequency of interest), makes it possible to model the maximum field statistically [1], and the corresponding frequency should be covered in the overmoded regime (the low frequency limit no less than a mode count of 60). Specifically, the Cartesian field components sampled from RC follow a Rayleigh distribution, and thus the power is exponentially distributed, the maximums can then be described by the extreme value statistics [2]. For a given RC with the same input power, however, the power received by

antenna relies on the number of independent samples when using the extreme value theory; that is, the estimated maximum field will have no upper bound especially for the unconditional probability density functions (PDFs) [3]-[6]. Therefore, the extreme value statistics may not be applicable as the estimates are contrary to common sense physics. Regarding low frequencies (i.e., low mode densities), there is no universally accepted mathematical model that sufficiently describes the field distribution corresponding to the undermoded frequencies (or even close to the lowest usable frequency of RC).

From the perspective of the tail behaviors of the empirical distribution, the generalized extreme value (GEV) theory based framework can be used to model the maximum field directly. It is easy to demonstrate that the exponential distribution converges to the maximum domain of attraction (MDA) of GEV distribution with shape parameter $k \rightarrow 0$ (i.e., the *Gumbel* type) [7]. Moreover, a large number of measurements have revealed that the results sampled at undermoded, weakly- and highly-overmoded frequencies show a good fitting with GEV distribution of $k > 0$ (fat tail, the *Fréchet* type), $k \rightarrow 0$ and $k < 0$ (thin tail, the *reverse Weibull* type), respectively [3], [5], [8], [9]. Without any doubt, the resonance modes with increasing frequency provide a more reasonable explanation for tail behaviors of

these samples. At low frequencies, it is really difficult to capture the samples related to the resonances, resulting in a significant fat tail in the empirical distribution, while the scattering of electromagnetic waves in a chaotic manner makes the resonances easier to be sampled, accounting for the thin tail at high frequencies.

Of particular note is that the samples should be independent and identically distributed (*i.i.d.*) for GEV distribution, thus requiring the mode-stirred techniques to be carried out within electrically large enclosures, e.g., the mechanical stirrer in RCs. However, for arbitrary electrically large enclosures, e.g., below-deck compartments in ships, ammunition containers in bunkers, aircraft cabins and bays [10], [11], the mechanical stirrer is not easy to be installed like that for RCs. According to the solution of scalar Green's function, fortunately, it has been verified that the frequency stirring (FS) also offers good field uniformity, being regarded as an alternative for mechanical stirring (MS) [12]. Fundamentally, FS can provide sufficient numbers of *i.i.d.* samples, which have been applied for electromagnetic shielding effectiveness (SE) evaluation in nested RCs using GEV distribution [13].

The aim of this work is therefore to model the maximum electromagnetic field (EMF) for arbitrary electrically large enclosures covering the undermoded and the overmoded frequency regimes. To simplify the testing procedure, a vector network analyzer (VNA) is used for FS, the *i.i.d.* samples are recorded to extract the maximums intended for the estimation of unknown parameters in GEV distribution, and then we can assess the maximum EMF in the case of a desired confidence interval. To verify the maximums estimated by GEV distribution, we also focus on the comparison of:

- i. The parameters in GEV distribution estimated by FS and MS, respectively, and the corresponding maximum EMF with a given 95 % confidence interval. Indeed, the hybrid stirring (FS+MS) is more useful to model the maximum EMF with GEV, which can sample a sufficient number of maximums and reduce the measurement uncertainty. Herein, the main aim is to show the comparisons between using and not using MS, the hybrid stirring (FS+MS) is not the focus of attention (more details about the comparisons between MS and hybrid stirring can be found in [14]).
- ii. The maximum EMF estimated by GEV distribution and IEC 61000-4-21 only for the overmoded frequency regime.

The rest of this paper is structured as follows. In Section 2, the GEV theory, including the distribution function and the parameter estimation method, is presented. In Section 3, the measurement configuration is described. In Section 4, the experimental results are given with a comparison of the maximum EMF estimated by different methods. And finally, Section 5 concludes this work.

2. THEORY

A. GEV distribution

Let $\xi_{1,N}, \xi_{2,N}, \dots, \xi_{n,N}$ be the N th set of n *i.i.d.* random variables with cumulative distribution function (CDF) $F(x)$, and the corresponding maximum is $\left[\xi_n \right]_N = \max_{i \in \mathbb{N}} \xi_{i,N}$.

Assume that there exist linear normalizing sequences $\{a_N > 0\}$ and $\{b_N\}$ for all N maximums such that $F(x)$ converges to the MDA of GEV distribution $G(x)$, namely [7]

$$G = F^n \Rightarrow \lim_{n \rightarrow \infty} [F(a_N x + b_N)]^n \rightarrow G(x) \quad (1)$$

According to the Fisher-Tippett theorem, $G(x)$ can be one of the following three types: *Fréchet* ($k > 0$), *Gumbel* ($k \rightarrow 0$), and *reverse Weibull* ($k < 0$). More precisely, the three types are combined in a unified form called GEV distribution $G_{\text{GEV}}(x)$ as [7]

$$G_{\text{GEV}}(x) = \begin{cases} \exp \left\{ - \left(1 + k \frac{x-m}{s} \right)^{-\frac{1}{k}} \right\}, & k \neq 0 \\ \exp \left\{ - \exp \left(- \frac{x-m}{s} \right) \right\}, & k = 0 \end{cases} \quad (2)$$

where k , s and m indicate the shape, scale and location parameters, respectively.

To provide intuitive explanation for the tail behavior of GEV distribution and the maximum field, herein we show a simple case as depicted in Fig.1.

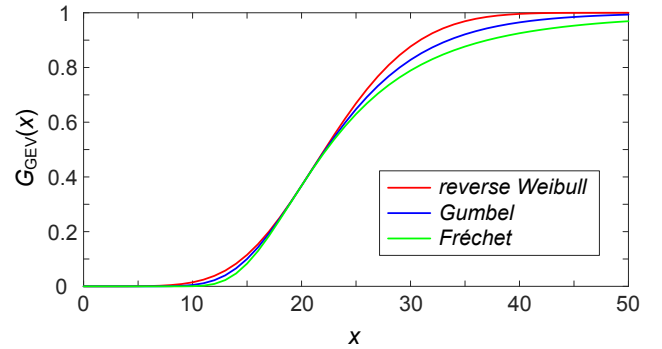


Fig.1. GEV distribution for $s = 4$, $m = 10$, and $k = -0.2$ (*reverse Weibull*), 0 (*Gumbel*), 0.2 (*Fréchet*).

As mentioned in the Introduction, for undermoded frequencies, e.g., the *Fréchet* type as shown in Fig.1., there is a significant fat tail for the CDF; that is, the maximum field cannot be easily captured in the case of the sparse resonance modes. While for overmoded frequencies, especially the case of *reverse Weibull* type, a sufficient number of modes will make the maximum field to be easily captured, and thus resulting in the thin tail in Fig.1.

B. Parameter estimation method

In general, the moment estimation (ME) and the maximum likelihood estimation (MLE) are commonly used methods for assessing the unknown parameters in the empirical distribution. For the maximum field in RCs, the samples essentially have an uncertainty within 3 dB at overmoded frequencies. Therefore, when calculating high-order moments for ME, e.g., the 2nd moment for the *Gumbel* type with 2 unknown parameters, the 3rd moment for the *Fréchet* and the *reverse Weibull* type with 3 unknown parameters, the uncertainty will inevitably be amplified, resulting in large uncertainty for these estimated parameters, despite the same frequency. As for MLE, a sufficient number of *i.i.d.*

maximums (generally $N \geq 50$) should be sampled to ensure that these parameters are asymptotically unbiased. However, as discussed in [15], due to the mode density as well as the efficiency of mode-stirred wall, it is really difficult to obtain enough independent samples, especially at low frequencies.

In view of these issues, the L-moments (L-Ms) method is used in this work, which can be regarded as an alternative for small samples in many applications [3], [13], [16].

For the set of N maximums $[\xi_n]_1, [\xi_n]_2, \dots, [\xi_n]_N$, we can define an ordered sample $x_1 \leq x_2 \leq \dots \leq x_N$, where $x_1 = \min_{i \in N} [\xi_n]_i$, and $x_N = \max_{i \in N} [\xi_n]_i$. As per [3] and [16], we can estimate the L-Ms l_1 , l_2 , and l_3 , namely

$$\begin{aligned} l_1 &= b_0 \\ l_2 &= 2b_1 - b_0 \\ l_3 &= 6b_2 - 6b_1 + b_0 \end{aligned} \quad (3)$$

where b_0 , b_1 , and b_2 are the parameters derived by the ordered sample,

$$\begin{cases} b_0 = \sum_{i=1}^N \frac{x_i}{N} \\ b_1 = \sum_{i=1}^N \frac{(i-1)x_i}{N(N-1)} \\ b_2 = \sum_{i=1}^N \frac{(i-1)(i-2)x_i}{N(N-1)(N-2)} \end{cases} \quad (4)$$

Then, the unknown parameters in GEV distribution are [3]

$$\begin{aligned} \hat{k} &= -7.859z - 2.5994z^2 \\ \hat{s} &= \frac{-l_2}{(1-2\hat{k})\Gamma(1-\hat{k})} \hat{k} \\ \hat{m} &= l_1 + \frac{\hat{s}}{\hat{k}} \left(1 - \Gamma(1 - \hat{k})\right) \end{aligned} \quad (5)$$

with

$$z = \frac{2l_2}{3l_2 + l_3} - \frac{\ln 2}{\ln 3} \quad (6)$$

where $\Gamma(\cdot)$ is the Gamma function. For the sake of brevity, we can also use the *lmom* function defined in [17].

3. MEASUREMENT SETUP

The measurement was carried out in an aluminum enclosure with the interior dimensions of $0.493 \text{ m} \times 0.389 \text{ m} \times 0.294 \text{ m}$, and the theoretical fundamental resonance of about 491 MHz. The enclosure is equipped with a mechanical stirrer, rotating about a vertical axis within a cylindrical volume of 0.26 m height and 0.11 m diameter.

The test configuration is shown in Fig.2. A two-port VNA, model Rohde & Schwarz ZNB 20, is used together with a pair of 10 cm monopole antennas (being considered as the transmit (Tx) and receive (Rx) antennas, respectively). Rx antenna was placed at the working volume of enclosure and pointed at the stirrer. To minimize the direct coupling, Tx and Rx antennas were placed mutually orthogonal to each other.

The frequency range was set from 500 MHz to 6 GHz with a frequency step of 100 kHz, while the stirrer stepped 48 positions; the port power of VNA was set to 0 dBm. For either

position of mechanical stirrer, 55001 sets of S_{21} data were sampled. To the best of our knowledge, the S_{21} is oversampled with respect to 100 kHz, and thus it is inferred that most of the resonances can be recorded.

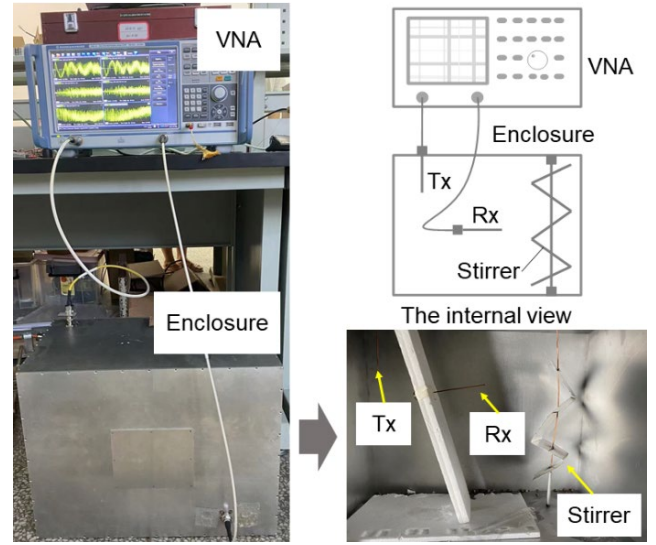


Fig.2. Experimental configuration.

4. RESULTS AND DISCUSSION

A. GEV parameters estimated by FS and MS configurations

To provide an estimate of the parameters (i.e., k , s , and m) in (2), one should extract N maximums from the measurements. For FS related configuration, the stirring bandwidth (BW) should be rather carefully selected. At low frequencies, there may be no mode excited in the stirring bandwidth, resulting in incorrect estimation of the parameter k (more details are explained in [13]). Herein, BW is set as 20 MHz, and the step frequency is 400 kHz to ensure a sufficient number of independent frequencies; that is, $N = 51$ sets of maximums are used to assess the parameters in the empirical distribution.

As for MS, these 48 stirring positions may be not all independent, and consequently one can reshape the array of size 48 into 4×12 stirrer positions, then $N = 12$ sets of maximums are extracted. It should be noted here that the estimate of parameter k is barely affected despite the existence of correlated samples in these maximums. It can be easily explained that the estimate of k is mainly contributed by resonances. For lower frequencies, there are almost no samples correlated with the extracted 12 sets of maximums in case of the sparse mode, thus will not affect the sign of k . For higher frequencies, whether the maximums relate to the same resonance or not, it will also not affect the estimation of k . When compared with FS, however, the parameter s (being the variable related to the standard deviation of the maximums) estimated by MS is larger (for the overall frequencies) due to the insufficient number of independent samples.

To estimate the parameters k , s , and m in (2), L-Ms method is used for maximums extracted by FS and MS configurations, respectively, and the corresponding results are shown in Fig.3. As discussed in this section, the incorrect estimation of parameter k is mainly concentrated in the

undermoded frequencies, since no mode can be excited within the BW for FS, or the stirring procedure for MS. Moreover, fewer numbers of independent maximums also confirm that the MS configuration has a greater uncertainty, resulting in a larger s , as shown in Fig.3.

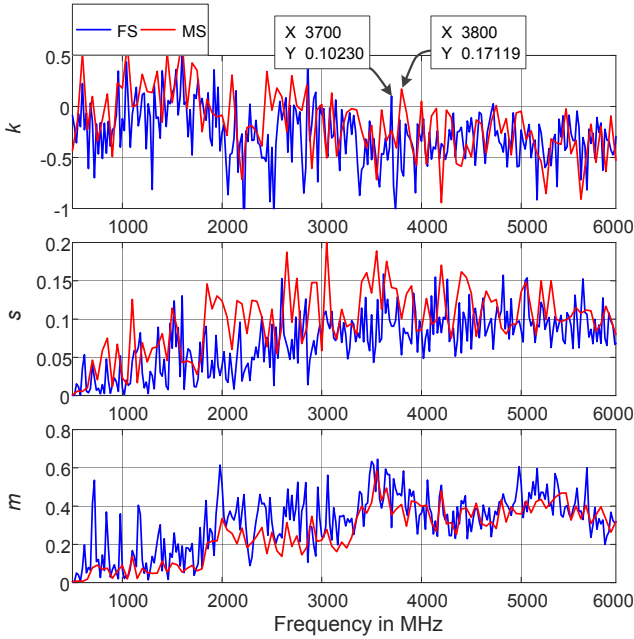


Fig.3. GEV parameters (k , s , and m) estimated by FS data and MS data, respectively.

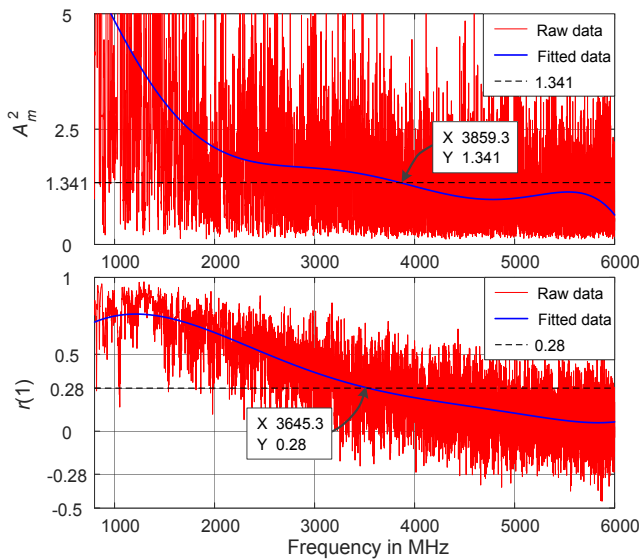


Fig.4. The frequency estimated by the “well stirred condition” (more details about the method can be found in [18]).

Of particular note is that both FS and MS configurations can be used to point out the asymptotic state discriminated EMF behavior between the undermoded and the overmoded frequencies. In fact, as mentioned in the Introduction, the shape parameter k can also be regarded as an indicator for revealing the undermoded frequencies tending to those weakly- or highly-overmoded. As shown in Fig.3., the prudently estimated frequency, used to define the EMF

behavior converging from undermoded to weakly- or highly-overmoded, is 3700 MHz for FS, and 3800 MHz for MS. As per [18], we can also use the “well stirred condition” to determine the frequency, i.e., the larger estimated by Anderson–Darling goodness-of-fit test (with a hypothesis that the samples follow the Rayleigh distribution) and by the sample correlation. For the sake of brevity, Fig.4. shows the frequency determined by the Anderson–Darling statistics A_m^2 (the threshold is 1.341 for Rayleigh [19], [20]) and the first-order autocorrelation coefficient $r(1)$ (the threshold is 0.28 [18]), and obviously the larger is 3859.3 MHz, validating the conservative estimates of the EMF behavior with GEV distribution.

B. The maximum EMF

Referring to the GEV distribution, we can estimate the maximums by the quantile $x_p = G_{\text{GEV}}^{-1}(p)$, ($0 < p < 1$), i.e.,

$$x_p = \begin{cases} m - s/k (1 - (-\ln p)^{-k}), & k \neq 0 \\ m - s \ln(-\ln p), & k = 0 \end{cases} \quad (7)$$

It is worth noting that we use the maximum S_{21} samples to estimate the GEV parameters (k , s , and m) for FS and MS configurations, thus the quantile x_p in (7) is the estimated maximum of S_{21} . To well model the maximum EMF, we should correct with the mismatch coefficients, e.g., S_{11} and S_{22} . As discussed in [5], the maximum EMF E_{\max_p} can be derived by

$$E_{\max_p} = \frac{4\pi}{\lambda} \sqrt{\frac{5\pi}{\eta_{\text{Tx}}\eta_{\text{Rx}}} \cdot \frac{x_p}{(1-|S_{11}|^2)(1-|S_{22}|^2)}} \cdot P_{\text{in}} \quad (8)$$

where λ is the wavelength, η_{Tx} and η_{Rx} are the antenna efficiency of Tx and Rx, respectively, P_{in} is the input power of the enclosure.

As for IEC 61000-4-21, the maximum EMF E_{\max} is derived from the extreme value statistics [2], [21], [22], namely

$$E_{\max} = \left(\frac{4\pi}{\lambda} \sqrt{\frac{5\pi}{\eta_{\text{Tx}}\eta_{\text{Rx}}} \cdot \frac{\langle |S_{21}|^2 \rangle}{(1-|S_{11}|^2)(1-|S_{22}|^2)}} \cdot P_{\text{in}} \right) \cdot \alpha(N) \quad (9)$$

where the symbol $\langle \rangle$ denotes the overall average, $\alpha(N)$ is the function of N as defined in [22]. And specifically, $\alpha(N) = 1.95$ for $N = 12$, and $\alpha(N) = 2.36$ for $N = 50$. For the sake of brevity, we can define ζ as

$$\zeta = E_{\max} \sqrt{\eta_{\text{Tx}}\eta_{\text{Rx}}(1-|S_{11}|^2)(1-|S_{22}|^2)} \quad (10)$$

Considering a desired confidence of 95 %, the confidence interval $[x_{0.025}, x_{0.975}]$ is used to assess the maximums with GEV distribution. As shown in Fig.5., the maximums related to FS and MS configurations show a good agreement for 500 MHz to 6 GHz. It can be concluded that FS configuration is a good solution to evaluate the maximum EMF for the arbitrary electrically large enclosures without a mechanical stirrer.

At frequencies above the 60th resonance, i.e., 1.5 GHz for the case in Fig.2., ζ relies on the number of independent maximums N , while as discussed in [5], the confidence

interval of the maximum EMF is barely affected by N . Therefore, for the arbitrary electrically large enclosures, GEV distribution can be used to assess the maximum EMF with a desired confidence.

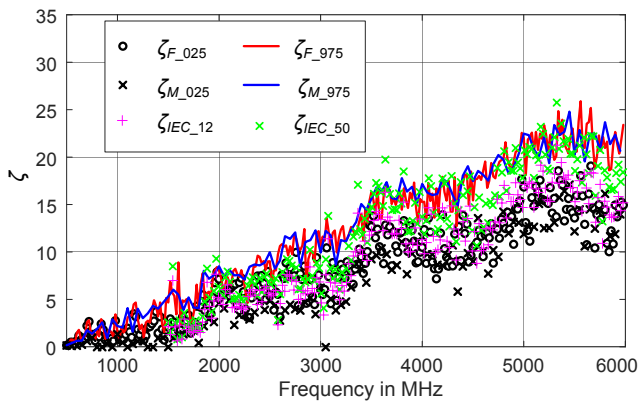


Fig.5. Comparison of maximums estimated by GEV distribution and IEC 61000-4-21. Specifically, $\zeta_{F,025}$ and $\zeta_{M,025}$ are the values related to $x_{0.025}$ in FS and MS configurations, respectively, and similarly $\zeta_{F,975}$ and $\zeta_{M,975}$ are related to $x_{0.975}$. The values $\zeta_{IEC,12}$ and $\zeta_{IEC,50}$ derived by (9) rely on $N = 12$ and $N = 50$, respectively.

5. CONCLUSION

In this work, we have shown how to model the maximum EMF for arbitrary electrically large enclosures using the GEV distribution and FS configuration. For this purpose, we make a comparison between the parameters in GEV distribution for both FS and MS configurations, and a comparison between the maximum EMF estimated by GEV distribution and IEC 61000-4-21. The results show that FS configuration can be regarded as a good solution to evaluate the maximum EMF for the arbitrary electrically large enclosures without a mechanical stirrer, and GEV distribution can be used to assess the maximum EMF with a desired confidence.

REFERENCES

- [1] Hill, D.A. (1998). Plane wave integral representation for fields in reverberation chambers. *IEEE Transactions on Electromagnetic Compatibility*, 40 (3), 209-217. <https://doi.org/10.1109/15.709418>
- [2] Ladbury, J., Koepke, G., Camell, D. (1999). *Evaluation of the NASA langley research center mode-stirred chamber facility*. NIST Technical Note 1508.
- [3] Orjubin, G. (2007). Maximum field inside a reverberation chamber modeled by the generalized extreme value distribution. *IEEE Transactions on Electromagnetic Compatibility*, 49 (1), 104-113. <https://doi.org/10.1109/TEMC.2006.888172>
- [4] Gifuni, A. (2011). Deterministic approach to estimate the upper bound of the electric field in a reverberation chamber. *IEEE Transactions on Electromagnetic Compatibility*, 53 (3), 570-578. <https://doi.org/10.1109/TEMC.2010.2102359>
- [5] Hu, P., Zhou, Z., Zhou, X., Sheng, M. (2020). Maximum field strength within reverberation chamber: A comparison study. In *6th Global Electromagnetic Compatibility Conference (GEMCCON)*. IEEE. <https://doi.org/10.1109/GEMCCON50979.2020.9456734>
- [6] Hu, P., Zhou, X., Zhou, Z. (2020). On the modelling of maximum field distribution within reverberation chamber using the generalized extreme value theory. In *IEEE MTT-S International Conference on Numerical Electromagnetic and Multiphysics Modeling and Optimization (NEMO)*. IEEE. <https://doi.org/10.1109/NEMO49486.2020.9343522>
- [7] Coles, S. (2001). *An Introduction to Statistical Modeling of Extreme Values*. Springer, 46-48. <https://doi.org/10.1007/978-1-4471-3675-0>
- [8] Gradoni, G., Arnaut, L.R. (2010). Generalized extreme-value distributions of power near a boundary inside electromagnetic reverberation chambers. *IEEE Transactions on Electromagnetic Compatibility*, 52 (3), 506-515. <https://doi.org/10.1109/TEMC.2010.2043107>
- [9] Nourshamsi, N., West, J.C., Hager, C.E., Bunting, C.F. (2019). Generalized extreme value distributions of fields in nested electromagnetic cavities. *IEEE Transactions on Electromagnetic Compatibility*, 61 (4), 1337-1344. <https://doi.org/10.1109/TEMC.2019.2911927>
- [10] Tait, G.B., Slocum, M.B., Richardson, R.E. (2009). On multipath propagation in electrically-large reflective spaces. *IEEE Antennas and Wireless Propagation Letters*, 8, 232-235. <https://doi.org/10.1109/LAWP.2009.2014572>
- [11] Tait, G.B., Richardson, R.E., Slocum, M.B., Hatfield, M.O., Rodriguez, M.J. (2011). Reverberant microwave propagation in coupled complex cavities. *IEEE Transactions on Electromagnetic Compatibility*, 53 (1), 229-232. <https://doi.org/10.1109/TEMC.2010.2051442>
- [12] Hill, D.A. (1994). Electronic mode stirring for reverberation chambers. *IEEE Transactions on Electromagnetic Compatibility*, 36 (4), 294-299. <https://doi.org/10.1109/15.328858>
- [13] Hu, P., Zhou, Z., Zhou, X., Li, J., Ji, J., Sheng, M. (2020). Generalized extreme value distribution based framework for shielding effectiveness evaluation of undermoded enclosures. In *International Symposium on Electromagnetic Compatibility - EMC EUROPE*. IEEE. <https://doi.org/10.1109/EMCEUROPE48519.2020.9245665>
- [14] Hu, P. (2021). *Study on radiated susceptibility tests using mode-stirred reverberation chambers*. Doctoral dissertation, Southeast University, Nanjing, China.
- [15] Zhou, Z., Hu, P., Zhou, X., Ji, J., Sheng, M., Li, P., Zhou, Q. (2020). Performance evaluation of oscillating wall stirrer in reverberation chamber using correlation matrix method and modes within Q-bandwidth. *Transactions on Electromagnetic Compatibility*, 62 (6), 2669-2678. <https://doi.org/10.1109/TEMC.2020.2983981>
- [16] Hosking, J.R., Wallis, J.R. (1997). *Regional Frequency Analysis: An Approach Based on L-Moments*. Cambridge University Press. <https://doi.org/10.1017/CBO9780511529443>

- [17] Bekker, K.N. (2004). Imom.m. *MATLAB Central File Exchange*.
<https://www.mathworks.com/matlabcentral/fileexchange/5874-lmom-m>
- [18] Andrieu, G., Ticaud, N., Lescoat, F., Trougnou, L. (2019). Fast and accurate assessment of the “Well Stirred Condition” of a reverberation chamber from S11 measurements. *IEEE Transactions on Electromagnetic Compatibility*, 61 (4), 974-982.
<https://doi.org/10.1109/TEMC.2018.2847727>
- [19] Stephens, M.A. (1974). EDF statistics for goodness of fit and some comparisons. *Journal of the American Statistical Association*, 69 (394), 730-737.
<https://doi.org/10.1080/01621459.1974.10480196>
- [20] Lemoine, C., Besnier, P., Drissi, M. (2007). Investigation of reverberation chamber measurements through high-power goodness-of-fit tests. *IEEE Transactions on Electromagnetic Compatibility*, 49 (4), 745-755.
<https://doi.org/10.1109/TEMC.2007.908290>
- [21] Romero, S.F., Gutierrez, G., Gonzalez, I. (2014). Prediction of the maximum electric field level inside a metallic cavity using a quality factor estimation. *Journal of Electromagnetic Waves and Applications*, 28 (12), 1468-1477.
<https://doi.org/10.1080/09205071.2014.929049>
- [22] Xu, Q., Chen, K., Shen, X., Li, W.H., Zhao, Y.J., Huang, Y. (2019). Comparison of the normalized maximum field strength using E-field probe and VNA methods in a reverberation chamber. *IEEE Antennas and Wireless Propagation Letters*, 18 (10), 2135-2139.
<https://doi.org/10.1109/LAWP.2019.2938833>

Received November 11, 2021

Accepted April 28, 2022